Journal of General Virology (2009), **90**, 95–104 DOI 10.1099/vir.0.005512-0

Adenovirus type 5 E4 Orf3 protein targets promyelocytic leukaemia (PML) protein nuclear domains for disruption via a sequence in PML isoform II that is predicted as a protein interaction site by bioinformatic analysis

Keith N. Leppard,[1] Edward Emmott,[1]† Marc S. Cortese[2] and Tina Rich[2]

[1]Department of Biological Sciences, University of Warwick, Coventry CV4 7AL, UK

[2]Institute of Comparative Medicine, University of Glasgow, Glasgow G61 1QH, UK

Correspondence
Keith N. Leppard
Keith.Leppard@warwick.ac.uk

Received 10 July 2008
Accepted 10 September 2008

Human adenovirus type 5 infection causes the disruption of structures in the cell nucleus termed promyelocytic leukaemia (PML) protein nuclear domains or ND10, which contain the PML protein as a critical component. This disruption is achieved through the action of the viral E4 Orf3 protein, which forms track-like nuclear structures that associate with the PML protein. This association is mediated by a direct interaction of Orf3 with a specific PML isoform, PMLII. We show here that the Orf3 interaction properties of PMLII are conferred by a 40 aa residue segment of the unique C-terminal domain of the protein. This segment was sufficient to confer interaction on a heterologous protein. The analysis was informed by prior application of a bioinformatic tool for the prediction of potential protein interaction sites within unstructured protein sequences (predictors of naturally disordered region analysis; PONDR). This tool predicted three potential molecular recognition elements (MoRE) within the C-terminal domain of PMLII, one of which was found to form the core of the Orf3 interaction site, thus demonstrating the utility of this approach. The sequence of the mapped Orf3-binding site on PML protein was found to be relatively poorly conserved across other species; however, the overall organization of MoREs within unstructured sequence was retained, suggesting the potential for conservation of functional interactions.

INTRODUCTION

Human adenovirus type 5 (Ad5) is one of a diverse collection of viruses that interact during infection with nuclear structures termed ND10 or promyelocytic leukaemia (PML) protein nuclear domains (PML-NDs reviewed by Everett & Chelbi-Alix, 2007; Leppard & Dimmock, 2006). These structures are complex multi-protein assemblies within which PML is a key component, essential for the localization of other proteins to PML-NDs. PML-NDs have been implicated in a variety of important cell processes, including DNA damage and stress responses, senescence, apoptosis and innate immunity (Bernardi & Pandolfi, 2007).

The targeting of PML-NDs by viruses has been linked to avoidance of innate immune responses. The incoming genomes of several nucleus-replicating DNA viruses localize adjacent to PML-NDs (Ishov & Maul, 1996). For herpes simplex virus type 1 (HSV1), this has been shown to involve the mobilization of existing PML-ND components to the sites of virus ingress (Everett & Murray, 2005). Both HSV1 and human cytomegalovirus infections induce the gross disruption of PML-NDs and, for HSV1, degradation of the PML protein (Everett & Maul, 1994; Kelly *et al.*, 1995). Ad5 infection disrupts PML-NDs by deforming them into a large number of elongated tracks (Carvalho *et al.*, 1995; Doucas *et al.*, 1996). For both HSV1 and Ad5, mutations that prevent expression of the virus-coded PML-ND disruption function leave the viruses highly sensitive to innate and intrinsic antiviral responses (Everett *et al.*, 2006, 2008; Ullman & Hearing, 2008; Ullman *et al.*, 2007). Thus it has been proposed that PML-NDs or their components play a key role in the detection of virus infection and/or the subsequent cellular response and that consequently many viruses have evolved proteins that target and modify this PML-ND function.

The *pml* gene encodes six C-terminally variant nuclear PML protein isoforms (I–VI) that contribute to PML-ND formation and these are further modified by covalent attachment of SUMO proteins to up to three lysine residues within their common N-terminal domain (Fig. 1a)

†Present address: Institute of Molecular and Cellular Biology and Astbury Centre for Structural Molecular Biology, University of Leeds, Leeds LS2 9NZ, UK.

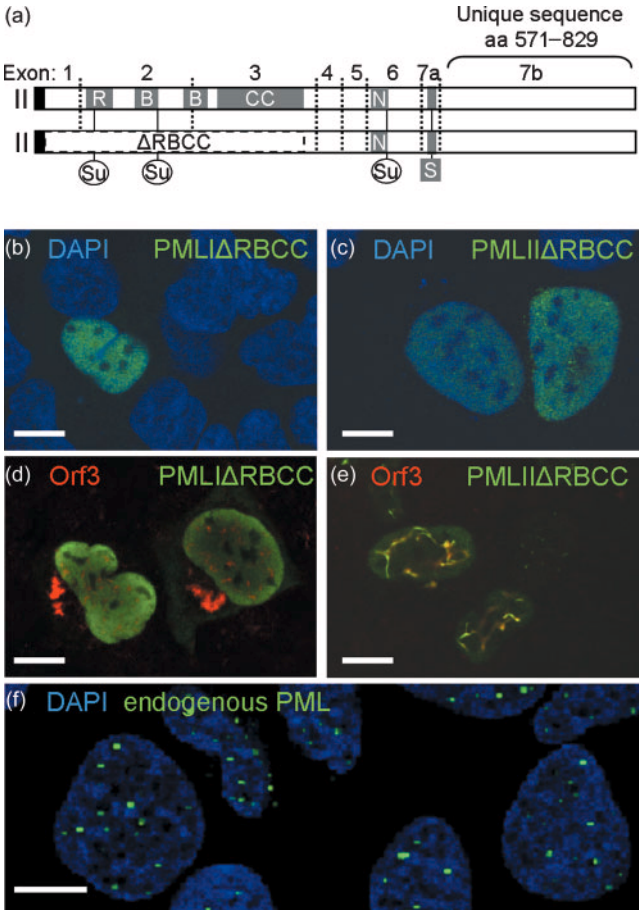

Fig. 1. PMLII–Orf3 interaction does not require the RBCC motif. (a) A schematic representation of PMLII (top) and its ΔRBCC variant (bottom). The RBCC domain comprises ring finger (R), two zinc-binding B boxes (B) and a coiled-coil region (CC). Also indicated are the PML nuclear localization signal (N), SUMO-binding site (S) and the three sites of covalent modification by SUMO1 (Su). The FLAG epitope N-terminal extension is shown as a black box. (b–f) Immunofluorescence analysis of U2OS cells either transfected with (b) FLAG-PMLIΔRBCC or (c) FLAG-PMLIIΔRBCC and stained for FLAG (green) and DNA (4,6-diamidino-2-phenylindole, DAPI, blue), transfected with (d) FLAG-PMLIΔRBCC and Orf3 or (e) FLAG-PMLIIΔRBCC and Orf3 and stained for FLAG (green) and Orf3 (red), or mock-transfected (f) and stained for endogenous PML (green) and DNA (DAPI, blue). Bars, 10 μm.

(Borden *et al.*, 1996; Fagioli *et al.*, 1992; Jensen *et al.*, 2001; Sternsdorf *et al.*, 1997). Assembly of PML into PML-NDs requires the N-terminal RBCC motif (Fig. 1a) (Borden *et al.*, 1996) and is thought to be mediated by non-covalent binding of attached SUMO groups to an interaction motif encoded by exon 7a and present in isoforms I–V (Shen *et al.*, 2006). The gene also encodes several cytoplasmic PML isoforms that lack the nuclear localization signal because of exon-skipping during mRNA splicing that have unique functions (Salomoni & Bellodi, 2007).

The Ad5 function that targets PML-NDs is the Orf3 protein, encoded by the E4 transcription unit, which draws PML into co-localization with it in characteristic tracks (Carvalho *et al.*, 1995; Doucas *et al.*, 1996). This Orf3 function is conserved among diverse human adenoviruses (Evans & Hearing, 2003), unlike its ability to reorganize the DNA repair complex, MRN, which is specifically a feature of Orf3 from species C human Ads (Stracker *et al.*, 2005). These two activities have been separated genetically. Recently, we showed that Orf3 targets PML-NDs via a specific and direct interaction with nuclear PML isoform II (PMLII) (Hoppe *et al.*, 2006). Mutations in Orf3 that abrogated its ability to bind PMLII also eliminated its ability to rearrange PML-NDs.

The aim of the present study was to define the sequences within PMLII that were responsible for binding Orf3. To achieve this, a targeted deletion strategy was employed, informed by both homology comparisons between PMLII proteins from three species and also the application of a predictive bioinformatic tool for identifying potential protein interaction sites within amino acid sequences (predictors of naturally disordered regions; PONDR). From the properties of these mutant proteins, a 40 aa segment of the PMLII C terminus was found to be necessary and sufficient for Orf3 binding. The propensity of this region of PMLII for protein interactions was independently predicted by PONDR analysis, demonstrating the utility of this approach to the mapping of protein–protein interactions.

METHODS

Plasmid cloning and mutagenesis. N-terminally FLAG-tagged PML cDNA clones in pCIneo expressing nuclear isoforms I–VI (Beech *et al.*, 2005), and an Ad5 E4 Orf3 expression plasmid (Hoppe *et al.*, 2006), have been described previously. The PML ΔRBCC deletion links the N-terminal FLAG epitope to PML residue 361, immediately distal to the RBCC motif. It was constructed by single-round PCR using FLAG-PML V template DNA with one primer bridging the FLAG–PML junction and the second complementary to PML exon 5. A restriction fragment containing the deletion was then used to replace the equivalent fragment in each of the pCIFLAG-PML cDNA clones. Specific deletions in PMLII ΔRBCC were constructed by a two-stage PCR protocol using two common primers complementary to PML exon 6 and the vector distal to the cDNA insert, and pairs of mutagenic primers designed to fuse the coding sequence in-frame at the desired location. Restriction fragments from second round PCR products were substituted for the corresponding wild-type sequence encoding aa 555 to the C terminus within PMLII ΔRBCC. To construct a green fluorescent protein (GFP) expression clone tagged with PMLII-derived sequences, plasmid phrGFP-N1 (Stratagene) was first modified to tag the hrGFP C terminus with the SV40 large T antigen nuclear localization signal, GPKKKRKVG (Kalderon *et al.*, 1984), and designated phrGFP-NLS. The sequence encoding PMLII aa 645–684 was amplified by PCR incorporating a *Bgl*II site at the N-terminal end and a stop codon plus *Eco*RI restriction site at the C-terminal end, suitable for cloning in-frame into phrGFP-NLS to generate phrGFP-NLS-m1m2. All clones were verified by DNA sequencing; primer sequences are available on request.

Cells and transfection. U2OS human osteosarcoma cells were maintained in McCoy's 5A medium (Gibco) supplemented with 10 % fetal bovine serum. Transfections of plasmid DNA were carried out using Lipofectamine 2000 (Invitrogen), with DNA lipid complexes formed at a ratio of 2 μl per 1 μg according to the manufacturer's instructions.

Immunofluorescence analysis. Cells (2.5×10^5) were grown on coverslips in 12-well culture plates, transfected 24 h later with 200 ng PML plasmid plus either 200 ng Orf3 plasmid or empty vector, and 24 h later fixed for 10 min with 10 % formalin in PBS and permeabilized for 10 min with 0.5 % Nonidet P40 in PBS. After blocking non-specific protein interactions with PBS containing 1 % (w/v) BSA for 1 h, antigens were then detected by sequential 1 h incubations with primary and secondary antibodies as follows: FLAG-tagged proteins, mouse monoclonal antibody (mAb) M2 (Sigma) and Alexa Fluor 488 goat anti-mouse IgG (Invitrogen); endogenous PML, mouse mAb PGM3 (Santa Cruz) and Alexa Fluor 488 goat anti-mouse IgG (Invitrogen); Ad5 E4 Orf3, rat mAb 6A11 (Nevels *et al.*, 1999) and Alexa Fluor 546 goat anti-rat IgG (Invitrogen). Bound antibodies or GFP were imaged using a Leica SP5 confocal microscope and data exported as TIF images. All images presented are single *z*-sections through the centre of the nucleus.

Co-immunoprecipitation and Western blot analysis. This was carried out as described previously (Hoppe *et al.*, 2006). Briefly, 3.5×10^6 U2OS cells plated on 10 cm dishes were transfected 24 h later with 4 μg PML plasmid or empty vector, together with 4 μg Orf3 plasmid. Cell extracts were prepared 24 h later, a proportion was reserved for total protein analysis and the remainder immunoprecipitated using covalently coupled M2-agarose (Sigma). Antigens were detected in Western blot analysis using, for Orf3, rat mAb 6A11 (Nevels *et al.*, 1999) and, for FLAG-tagged PML, rabbit polyclonal anti-M2 (Sigma).

PONDR analysis. The PMLII sequence was analysed for disorder propensity using the PONDR VLXT (Romero *et al.*, 1997, 2001) provided by Molecular Kinetics and the VSL2 disorder predictor (Obradovic *et al.*, 2005) via web access at http://www.pondr.com and http://www.ist.temple.edu/disprot/predictorVSL2.php, respectively. Regions with the potential to undergo disorder to order structural transitions upon binding to a partner, termed molecular recognition elements (MoREs) (Oldfield *et al.*, 2005) or molecular recognition features (MoRFs) (Mohan *et al.*, 2006), are indicated by sharp downward spikes (order propensity) flanked by regions of disorder (PONDR scores >0.5). (PONDR is © 2004 by Molecular Kinetics, all rights reserved.)

PML gene homology alignments. GenBank was searched for annotated PML genes and then for DNA sequences homologous to human *pml* exon 7a. This sequence was chosen as a search target because it encodes SUMO binding (Shen *et al.*, 2006) and degron motifs (Scaglioni *et al.*, 2006) that are likely to be well conserved between species. Full or partial *pml* gene sequences were identified from 10 placental and one marsupial mammalian species (GenBank accession nos: *Homo sapiens*, NT_010194; *Pan troglodytes*, NW_001225242; *Macaca mulatta*, NW_001121176; *Canis familiaris*, NW_876294; *Felis catus*, AANG01142599; *Mus musculus*, NT_039474; *Rattus norvegicus*, NW_001084873; *Bos taurus*, NW_001494036; *Equus caballus*, NC_009144; *Sus scrofa*, NW_001886480; *Monodelphis domestica*, NW_001581855). Sequences were manually aligned (MEGALIGN module; DNASTAR) and anchored on their similarity to human exon 7a. In human *pml*, the 5′ end of exon 7b, which encodes the C-terminal 259 residues of PMLII, lies 642 bp from the 3′ end of exon 7a. Splice acceptor sites and open reading frames (ORF) able to encode proteins with clear similarity to human PMLII were found in very similar positions (636–674 bp from exon 7a) in seven cases. Of the remaining sequences, similarity to the 5′ end of human exon 7b was found in mouse and rat (1332 and 1171 bp from exon 7a, respectively) but the ORFs were scrambled by frame shifting mutations, while opossum had only a short intron from exon 7a to 8a (1966 bp compared with 7.5–10.7 kbp) with no discernible similarity to exon 7b. Eight predicted exon 7b-encoded polypeptides were aligned using the CLUSTAL V method. This alignment introduced two 2-position gaps into the 259 residue human PMLII sequence.

RESULTS

To show that the molecular target of E4 Orf3 within PML-NDs was PMLII, we previously co-expressed Orf3 with specific PML isoforms, in either co-immunoprecipitation or immunofluorescence co-localization analysis (Hoppe *et al.*, 2006). For the latter approach, we employed PML-null primary mouse embryo fibroblasts, since similar analysis in human cells was complicated by the presence of endogenous PMLs with which the transfected PML isoform could hetero-oligomerize. In order to test the interaction of transiently expressed PML variants with Orf3 in PML-containing human cells in this study, advantage was taken of the observation that the RBCC motif within the common N terminus of the nuclear PML isoforms (Fig. 1a) is necessary for these proteins to participate in PML-ND formation (Fagioli *et al.*, 1998). FLAG-tagged PML I–VI constructs lacking this motif were tested for their localization in U2OS cells either without or with co-expressed Orf3. All six ΔRBCC variants displayed an identical exclusively diffuse nuclear fluorescence when expressed alone, despite U2OS cells containing prominent PML-NDs formed of endogenous PML proteins (Fig. 1b, c and data not shown). This contrasts with the behaviour of the full-length isoforms, which are each recruited efficiently into PML-NDs (Beech *et al.*, 2005). When Orf3 was co-expressed with these proteins, only PMLIIΔRBCC was relocalized into tracks with Orf3 (Fig. 1d, e and data not shown), as expected from the earlier study. This result further showed that residues 1–360 of PMLII were dispensable for its interaction with Orf3.

In order to define further the PML sequences involved in Orf3 binding, a set of four in-frame deletions (Δ1–Δ4) was constructed in the unique C-terminal domain of FLAG-PMLIIΔRBCC. To inform the design of these deletions, three PMLII sequences annotated in GenBank databases, from human, chimpanzee and rhesus macaque, were compared. These sequences are highly conserved, but regions of lower conservation were identified and chosen as deletion end-points since these might be expected to lie between functional elements of the sequence (Fig. 2a). During construction of these mutations, we applied PONDR analysis to further inform mutational planning. This method predicts protein interaction motifs in protein sequence, based on the observation that proteins that are capable of multiple interactions are frequently highly disordered and that within this disorder there are short sequences that are predicted to have a propensity to adopt ordered structure. Well-defined dips in VLXT disorder

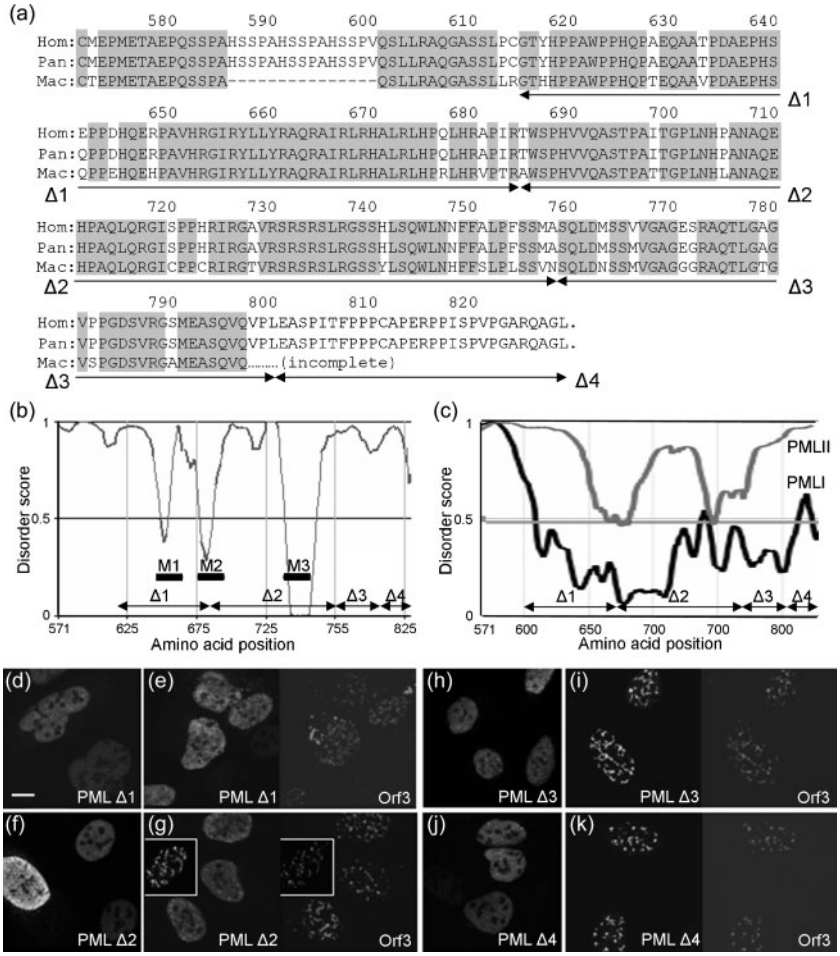

Fig. 2. Delineation of the Orf3-binding site in the C terminus of PMLII. (a) Amino acid sequence alignment of the exon 7b sequences of PMLII from human (Hom), chimpanzee (Pan) and macaque (Mac); grey shaded regions indicate identity between the three sequences. The beginning and end points of the in-frame deletion mutations Δ1–Δ4 generated in human PMLII cDNA are indicated below the alignment. (b) PONDR VLXT prediction for the C-terminal domain of PMLII, showing the predicted molecular recognition elements (MoRE) 1–3 relative to mutations Δ1–Δ4. (c) PONDR VLS2 prediction for the C-terminal domain of PMLII (grey) and PMLI (black). (d–k) Immunofluorescence analysis of U2OS cells transfected with (d) FLAG-PMLIIΔ1 alone or (e) with Orf3, (f) FLAG-PMLIIΔ2 alone or (g) with Orf3, (h) FLAG-PMLIIΔ3 alone or (i) with Orf3, (j) FLAG-PMLIIΔ4 alone or (k) with Orf3, and stained for FLAG and Orf3. Bar, 10 μm; all panels at this magnification.

prediction curves within disordered regions (disorder scores >0.5) can indicate short regions of order propensity (MoRE) that undergo disorder-to-order transitions upon binding to a partner. Previous studies have validated the use of these distinctive downward spikes in VLXT prediction curves to locate functional-binding regions (Oldfield *et al.*, 2005). The structural propensity of these short regions can be translated into a stable structure by interaction with an interacting partner (Bourhis *et al.*, 2004; Callaghan *et al.*, 2004; Longhi *et al.*, 2003).

The unique C-terminal sequence of PMLII, from aa 571, was analysed by two PONDR tools generating predictions VLXT and VSL2. The VLXT prediction (Fig. 2b) identified three potential MoREs within a region of predicted disorder that covered the entire PMLII C-terminal unique region, while the VSL2 prediction (which is based on a different and larger set of known structured and unstructured proteins) showed MoREs 1 and 2 as part of a single region of increased order propensity (Fig. 2c). By contrast, the PMLI C terminus was predicted to be more ordered with no MoREs (Fig. 2c), consistent with the fact that that this method of analysis is useful for finding sites of interaction within regions that are predominantly disordered, but not within ordered regions. PMLII MoRE1 lay within the Δ1 mutation, while MoRE3 was contained within Δ2; MoRE2 spanned the junction between Δ1 and Δ2.

The ability of PMLII ΔRBCC variants Δ1–Δ4 to associate with Orf3 was assessed by fluorescence co-localization. All four mutated proteins showed diffuse nuclear fluorescence when expressed alone (Fig. 2d, f, h, j). When co-expressed with Orf3, Δ3 and Δ4 showed complete co-localization in all cells (Fig. 2i, k), while Δ1 gave only diffuse nuclear fluorescence, lacking any co-localization ability (Fig. 2e). Δ2 showed an intermediate phenotype (Fig. 2g), with some cells demonstrating complete co-localization (Fig. 2g, inset), while the majority showed some co-localized tracks but with considerable residual diffuse nuclear fluorescence, suggesting that the ability of Δ2 to bind to Orf3 was impaired, but not completely abrogated. Thus, PML residues 615–684, including MoRE1 and part of MoRE2, are necessary for Orf3 binding, while sequences C-terminal of residue 685, including MoRE3, are not essential.

To map more precisely the sequences of PMLII necessary for the Orf3 interaction, and in the light of the PONDR predictions (Fig. 2b, c), five further in-frame deletions were constructed in the PMLII C terminus (Fig. 3a), removing either subsections of the region deleted in Δ1 (Δ7, Δ8 and

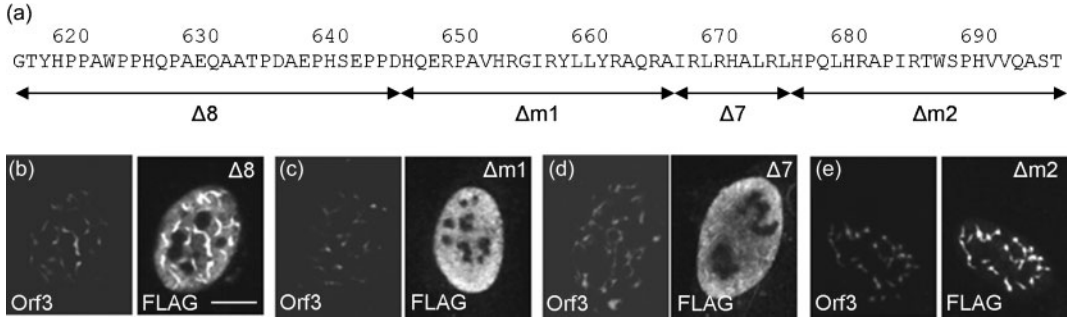

Fig. 3. Co-localization of PMLII with Orf3 requires sequences from MoRE1. (a) PMLII sequence across the MoRE1 and MoRE2 elements, showing the positions of deletion mutations as indicated. (b–e) Immunofluorescence analysis of U2OS cells transfected with Orf3 plus (b) PMLIIΔ8, (c) PMLIIΔm1, (d) PMLIIΔ7 and (e) PMLIIΔm2. Orf3 staining is shown on the left and FLAG (PML) staining on the right in each panel. Bar, 10 μm; all panels at this magnification.

Δm1), or the MoRE2 motif overlapping the boundary of Δ1 and Δ2 (Δm2); Δm1 and Δm2 were also combined in a double mutant (Δm1m2). When tested in the fluorescence co-localization assay, Δ8 and Δm2 strongly associated with Orf3 tracks (Fig. 3b, e), while Δm1, Δ7 and Δm1m2 were essentially unable to do so (Fig. 3c, d and data not shown); faint tracks of Δ7 were sometimes seen, but in contrast to Δ8 and Δm2 these only partially co-localized with Orf3. These data mapped the Orf3 interaction motif in PMLII to residues 645–674, with a possible supporting involvement of adjacent sequences from the properties of mutant Δ2 (Fig. 2g). This mapped region coincides almost exactly with the region of potential induced order (MoRE1/2) predicted in PMLII by PONDR VLXT and VSL2 (Fig. 2b, c).

To confirm that the induction of PML variant localization into Orf3 co-localized tracks was an indication of protein–protein interaction between these two partners, co-immunoprecipitation analysis was performed (Fig. 4). Each of the PML variants tested was efficiently expressed and precipitated by anti-FLAG agarose beads (Fig. 4a). However, although expression of Orf3 in the extracts was broadly equivalent across all samples (Fig. 4b), the amounts of Orf3 co-precipitated with the various FLAG-PMLs varied greatly (Fig. 4c). As expected, II ΔRBCC co-precipitated significant amounts of Orf3 (lane 4), while I ΔRBCC, included as a negative control, did not (lane 3). The Δ1, Δm1, Δm1m2 and Δ7 variants of II ΔRBCC did not co-precipitate Orf3 at all (lanes 5, 9, 11 and 12), consistent with the fact that these variants also failed to relocalize into tracks when co-expressed with Orf3 (Figs 2, 3 and data not shown). The other variants tested: Δ2, Δ3, Δ4, Δ8 and Δm2, each of which was able to associate with Orf3 by fluorescence analysis, also co-precipitated Orf3, in the case of Δ3 and Δ4 more efficiently than did the wild-type sequence. These results therefore confirm that PMLII residues 645–674, comprising the sequence deleted in Δm1 plus Δ7, are required for Orf3 binding.

To determine if these essential sequences from PMLII were also sufficient for Orf3 binding, PMLII residues 645–684, comprising MoRE1 and sequences C-terminal to it up to the original Δ1 boundary within MoRE2, were transferred onto the C terminus of hrGFP that was tagged with the nuclear localization signal from SV40 large T antigen to direct the protein to the nucleus; as expected, the location of hrGFP-NLS was unaffected by co-expression of Orf3 (Fig. 5a). Addition of the PMLII sequences caused the hrGFP fusion, expressed alone, to quantitatively relocalize

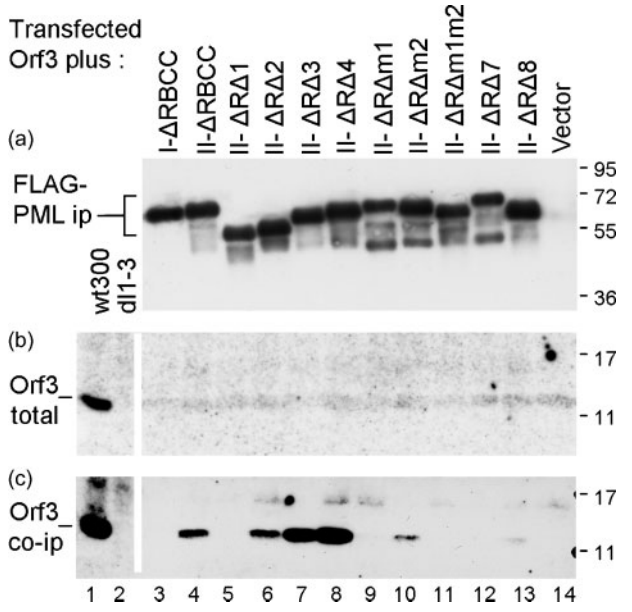

Fig. 4. Interaction of PMLII sequence variants with Orf3 by co-immunoprecipitation analysis. U2OS cells were co-transfected with Orf3 and FLAG-PML expression plasmids as indicated at the top of the figure and cell extracts prepared for total protein analysis and immunoprecipitation with anti-FLAG antibody. (a) Immunoprecipitated FLAG-PML, (b) Orf3 in total extract and (c) Orf3 co-immunoprecipitated with FLAG-PML. The migration positions of protein molecular mass markers (kDa) are shown at the right of each panel.

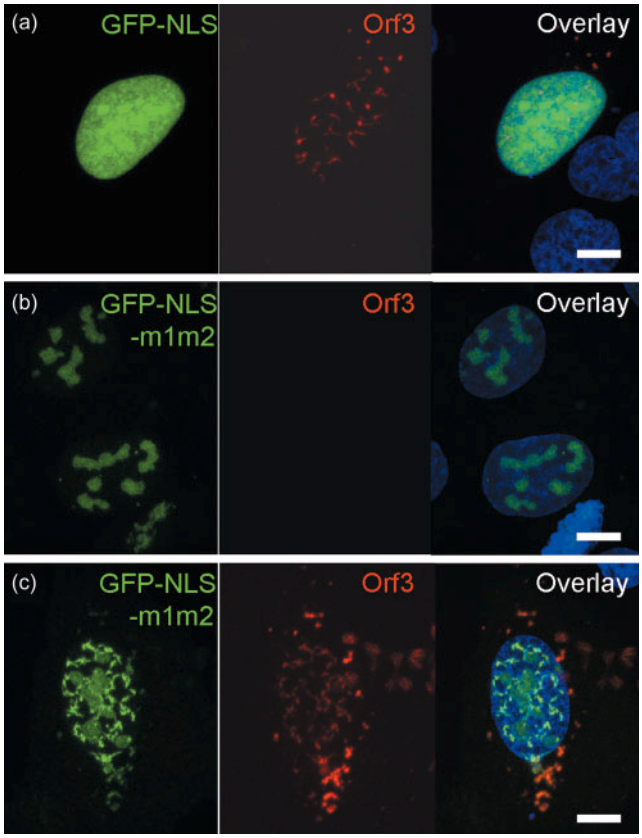

Fig. 5. PMLII residues 645–684 are sufficient for Orf3 binding. U2OS cells were transfected with (a) hrGFP-NLS plus Orf3, (b) hrGFP-NLS-m1m2 plus empty vector or (c) hrGFP-NLS-m1m2 plus Orf3 and then stained for Orf3 (red) and DNA (DAPI, blue). GFP fluorescence was visualized directly (green). Bars, 10 μm.

into structures that had the appearance of nucleoli (Fig. 5b). However, when Orf3 was co-expressed with this construct, a substantial fraction of the fusion protein was drawn back out of these structures into co-localization with Orf3 tracks (Fig. 5c), indicating that PMLII residues 645–684 were sufficient for Orf3 interaction and could function autonomously from the rest of the protein.

Having defined the Orf3-binding element in PMLII, we were interested to determine whether either its amino acid sequence or the position of MoREs within it was conserved among the PML proteins of different species. Seven of ten PML genes identified in database searches could be predicted to encode homologues of human PMLII. Of the other three, the exon 7b sequences in mouse and rat were non-functional, in agreement with experimental data for the mouse (Condemine *et al.*, 2006), while the opossum sequence lacked exon 7b completely. The extent of identity at each position in an alignment of human PMLII with these seven predicted PMLII C-terminal domains is represented in Fig. 6(a). Only 27 % of 263 positions were identical across seven or all eight of the sequences. This compares with 63 % of 267 positions in a similar alignment

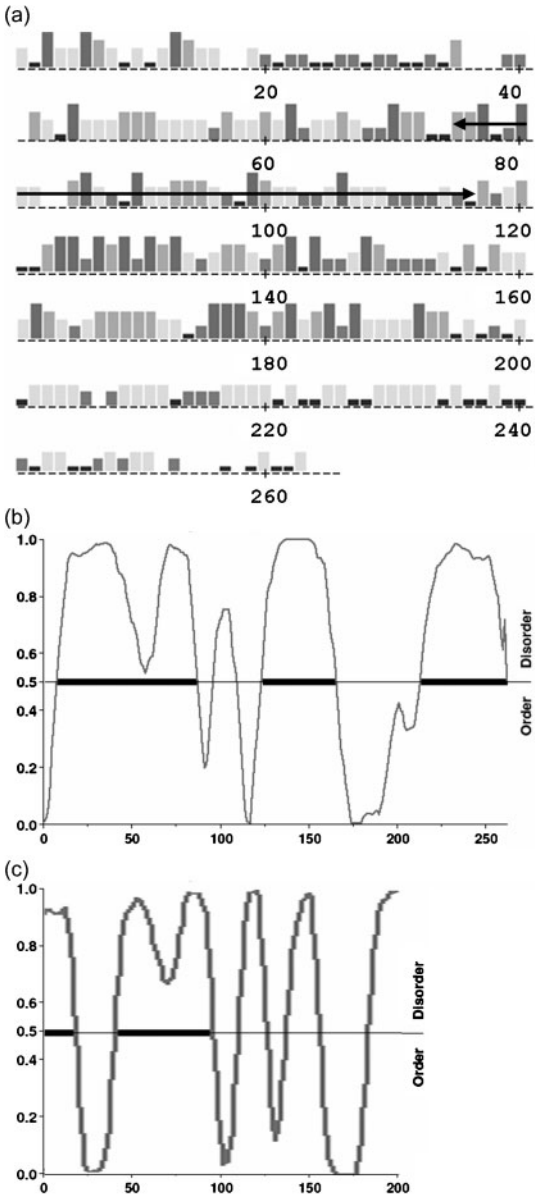

Fig. 6. Sequence and structure conservation in PMLII. (a) Sequence conservation across the predicted *pml* exon 7b-encoded polypeptides from human, chimpanzee, macaque, dog, cat, cow, horse and pig (see Methods for details). The bar height and shading indicate the extent of similarity at each position in the alignment, with the maximum bar height shown representing identity across all eight sequences and the next highest representing seven out of eight identity. The position of the 40 residue Orf3-binding sequence is represented by a black arrow. (b and c) PONDR VLXT predictions for the predicted C-terminal domains of bovine (b) and canine (c) PMLII.

of predicted PMLI C-terminal domains (substituting murine PML for feline PML sequence, since the feline exon 9 sequence was not available; data not shown). Thus the unique sequences of PMLII that are targeted by Ad5 are relatively poorly conserved in PML. Moreover, the mapped

Orf3 interaction sequence in PMLII did not coincide with the region of highest conservation (Fig. 6a, arrow).

PONDR VLXT analyses were then run for the predicted bovine (Fig. 6b) and canine (Fig. 6c) PMLII C termini. Despite the low sequence identity between the bovine and human sequences (45 % of 244 aligned positions where both have residues), three MoREs were predicted in bovine PMLII at positions very similar to those identified in the human protein. The canine PMLII exon 7b-encoded sequence is significantly shorter than the human form, being truncated at position 210 in the alignment. It too was predicted to contain several potential protein interaction sites, although their precise positions differed from those predicted for the human and bovine PMLII MoREs.

DISCUSSION

The Ad5 E4 Orf3 protein is required for the disruption of PML-NDs. This Orf3 function requires it to interact with PMLII (Hoppe *et al.*, 2006), a major component within the population of PML species in the cell (Condemine *et al.*, 2006). In this study, we have shown that the target for Orf3 binding is a 40 residue sequence within PMLII. Deletion of this sequence destroys the interaction with Orf3, whilst its transfer to a heterologous protein confers Orf3 interaction properties in an *in vivo* assay. The interacting PML sequence, residues 645–684, is encoded by exon 7b of the *pml* gene and is thus unique to PMLII among nuclear PML species, in full agreement with the observation that only this PML isoform can interact with Orf3.

The Orf3-binding sequence of PMLII was defined using cDNA clones deleted for the RBCC motif. The encoded proteins therefore lack the ability to hetero-oligomerize (Peng *et al.*, 2002) and so cannot be indirectly recruited into association with Orf3 via PML–PML interactions. As expected, they completely failed to localize into PML-NDs (Borden *et al.*, 1996), even though this cell type contained clearly defined PML-ND structures formed of endogenous PML with which the heterologous proteins were free to interact. Among the six nuclear PML isoforms, only the PMLII ΔRBCC derivative could associate with Orf3 in immunofluorescence or co-immunoprecipitation assays, in agreement with our previous study using full-length PMLII (Hoppe *et al.*, 2006) and indicating that the association of PMLII with PML-NDs is not necessary for its interaction with Orf3.

The various deletion variants of PMLII that retained Orf3 interaction ability did not always appear equivalent in activity. Although the fluorescence co-localization assay is not quantitative, it was consistently observed that the Δ3 and Δ4 mutants were effectively brought into Orf3 tracks as compared with the Δ2 mutant and even the undeleted PMLII C terminus. These same proteins were also more effective in co-precipitating Orf3. These data suggest that the C-terminal 70 residues of PMLII may exert a negative effect on its binding to Orf3. The other mutants that retained Orf3 interaction function, Δ2, Δ8 and Δm2, all appeared to be less efficiently recruited to Orf3 tracks, and for Δ8 and Δm2 this was supported by reduced co-immunoprecipitation of Orf3. Thus, the activity of the core Orf3-binding element in PMLII may be enhanced by its flanking sequences.

The use of deleted protein variants to map protein interactions has the caveat that such deletions may cause gross changes to the structure of the folded protein and hence impact on functions that are actually encoded elsewhere in the polypeptide. All of the C-terminally deleted PMLII variants used in the study accumulated to similar levels to undeleted PMLII, as judged by the strength of bands in Western blot analysis of total protein and the typical fluorescent intensity of individual expressing cells examined by immunofluorescence. Both these observations indicate that the deleted PMLII species were not destabilized relative to full-length protein and hence are not likely to be grossly altered in structure. The ability to express deleted forms of PMLII without such problems being manifested is likely due to the predicted disordered nature of the entire C-terminal domain.

The addition of the Orf3 interaction motif of PMLII onto hrGFP conferred apparent nucleolar targeting on the protein. PML has been shown previously to be induced into nucleolar localization by either DNA damage or inhibition of the proteasome (Bernardi *et al.*, 2004; Mattsson *et al.*, 2001) or to associate with nucleoli during normal growth of non-transformed cells (Janderová-Rossmeislová *et al.*, 2007). It is conceivable that our study has identified an element that contributes to this nucleolar targeting of endogenous PML proteins. However, it was shown recently that direct nucleolar targeting of PML was largely restricted to PML isoforms I and IV (Condemine *et al.*, 2007). Hence it is more probable that the nucleolar localization of hrGFP-M1M2 protein observed here results from the generation of activity through the transfer of this protein sequence into a heterologous context.

Orf3 reorganizes several cellular proteins in addition to PML, including RBCC family member TIF1α, which directly binds Orf3 (Yondola & Hearing, 2007), and the MRN complex comprising Mre11, Rad50 and Nbs1 (Stracker *et al.*, 2002). The direct-binding partner for Orf3 within MRN has not been determined, although Nbs1 is dispensable for Orf3 to relocalize Rad50 and Mre11 (Araujo *et al.*, 2005). The Orf3 sequence requirements for interaction with PML, MRN and TIF1α are very similar, suggesting that the Orf3-interaction sites in these proteins might be sequence-related. Similarity matches to the 40 residue Orf3-interaction motif from PMLII were identified in both Rad50 and TIF1α (Fig. 7). The significance of the Rad50 match is unclear, but the TIF1α match is clearly better than achieved in comparisons with two irrelevant proteins of similar length (T antigen, L4 100K). Moreover, the sequence match lies at the C-terminal end of the TIF1α RBCC domain, which has been shown to mediate Orf3

```
Rad50 (1312 aa):   901 LYREI-KDAK-EQVSPLETTLEK 921
                         |||.  :. :  :  .|:. |::
PMLII:  HQERPAVHRGIRYLLYRAQ-RAIRLRHALRLHPQLHRAPIR
                        |||. :  : ||||  ||
TIF1α (1050 aa):  375 LLYSKRLITYRLRHLLR 391

                        ||:.       :|::||
TIF1β (835 aa):   361 LLLSKKLIYFQLHRALK 377

                        |||:
SV40 large T:     170 LLYK 173   (708 aa)

                           ||: :.: ||::
Ad5 L4 100K:         189 RAD-KQLALRQG 199 (807 aa)
```

Fig. 7. Similarity alignments of the PMLII Orf3-binding motif with other proteins. Protein sequences [GenBank: AAB07119 (Rad50), NP_005582 (Mre11), NP_056989 (TIF1α), CAA66150 (TIF1β)] were analysed in pairwise alignments with the 40 residue Orf3-binding motif from PMLII (residues 645–684) using the Lipman–Pearson method, DNASTAR software (Ktuple 2; gap penalty 4; gap length penalty 12). Symbols '|: .' indicate identity and decreasing levels of similarity between each sequence and the PMLII motif.

binding (Yondola & Hearing, 2007). Finally, the corresponding sequence from its Orf3 non-interacting relative TIF1β (Yondola & Hearing, 2007) is significantly less similar to the PMLII Orf3-binding motif (Fig. 7). These strands of argument support the possibility that sequence relatedness with PMLII can predict the Orf3-binding site in TIF1α.

In addition to forming nuclear tracks, Orf3 also localizes to perinuclear cytoplasmic structures identified as aggresomes (Araujo *et al.*, 2005) and participates in delivering MRN complex to these structures for inactivation and degradation (Araujo *et al.*, 2005; Liu *et al.*, 2005). Here, Orf3 aggresomes were observed in only a minority of expressing cells. PML species unable to bind Orf3 never co-localized in these structures (e.g. Fig. 1d), while those variants able to bind Orf3 associated with aggresomes only in a few cells expressing high levels of the PML construct (data not shown). These data are consistent with the report that endogenous PML does not localize with Orf3 in aggresomes (Araujo *et al.*, 2005).

The mapped binding site for Orf3 in PMLII was found to be relatively poorly conserved between PML proteins of different species. Exon 7b, which encodes the unique portion of PMLII, was only found intact in a subset of species for which data were available, and for those species able to encode PMLII, its isoform-specific C-terminal sequence was considerably less well conserved than the equivalent region of PMLI. Moreover, even within the PMLII C terminus, the mapped interaction site was not the most conserved part of the sequence. These findings suggest that Ad5 Orf3 may not be able to interact widely with the PML proteins of other species. However, both the two non-human PMLII sequences for which PONDR analysis was carried out were predicted to contain MoREs and, for the bovine sequence, the position of these predicted elements was very similar to those predicted for human PMLII. Thus, it may be that Orf3 recognizes a shape or structure in PML rather than a highly specific sequence, in which case it may have wider cross-species binding reactivity than the sequence similarity analysis suggests. Whether Ad5 Orf3 can bind specifically to PMLII from other species remains to be tested.

Adenoviruses have been isolated from a wide range of animal species. Whilst these viruses retain the overall genome organization of the human Ads, including a presumptive E4 gene at the genome right end with multiple ORF, outside of the simian Ads it is not possible to identify definitive functional homologues of human Ad E4 Orf3 by sequence comparison. Thus, the host target(s) of Orf3 might be expected also to be quite divergent, assuming function has been conserved during the co-evolution of these viruses with their respective hosts. Given that the disruption of PML-NDs by Orf3 combats an intrinsic or innate antiviral response in human and primate cells (Ullman & Hearing, 2008; Ullman *et al.*, 2007), it will be interesting to explore the function of Ad5 Orf3 in other host species.

PONDR analysis identified three potential protein interaction sites (MoREs) within the C-terminal domain of human PMLII, one of which (MoRE1) formed the core of the Orf3-binding sequence subsequently identified. This study therefore demonstrates the potential for predicting functional protein-binding sites within unstructured polypeptide sequence by this method. The MoRE1 motif is unlikely to have evolved within PMLII to provide an interaction site for Orf3, given that the ability of the virus to make this interaction with the host can be seen as favouring the replication of virus and hence is likely to be deleterious to the host. Instead, it and the other two predicted MoREs are likely to have one or more endogenous cellular partners. The experimentally demonstrated ability of the C-terminal MoRE of p53 to bind four different partners (Oldfield *et al.*, 2008) serves as a model for how a viral protein could usurp an endogenous MoRE-mediated binding interaction and thereby alter normal cellular communication or protein function. Although MoREs do exhibit different degrees of specificity, their minimal-binding determinants facilitate promiscuity. If MoRE1 does have an endogenous partner, then its displacement by Ad5 Orf3 could contribute to the observed phenotype in relieving the antiviral response or to additional, as yet undetermined, phenotypes.

ACKNOWLEDGEMENTS

The authors gratefully acknowledge the assistance of G. Scott with cell culture and the DNA sequencing service provided by L. Ward, S. Davis and H. Brown in the Molecular Biology Core Facility, Department of Biological Sciences, University of Warwick. mAb specific for Ad5 E4 Orf3 was generously provided by Dr T. Dobner, Heinrich Pette Inst Expt Virol and Immunol, Martinistr 52, D-20251

Hamburg, Germany. This work was supported by grants from the Biotechnology and Biological Sciences Research Council to K. N. L. and to T. R., and from the AICR to M. C.

REFERENCES

Araujo, F. D., Stracker, T. H., Carson, C. T., Lee, D. V. & Weitzman, M. D. (2005). Adenovirus type 5 E4orf3 protein targets the Mre11 complex to cytoplasmic aggresomes. *J Virol* **79**, 11382–11391.

Beech, S. J., Lethbridge, K. J., Killick, N., McGlincy, N. & Leppard, K. N. (2005). Isoforms of the promyelocytic leukemia protein differ in their effects on ND10 organization. *Exp Cell Res* **307**, 109–117.

Bernardi, R. & Pandolfi, P. P. (2007). Structure, dynamics and functions of promyelocytic leukaemia nuclear bodies. *Nat Rev Mol Cell Biol* **8**, 1006–1016.

Bernardi, R., Scaglioni, P. P., Bergmann, S., Horn, H. F., Vousden, K. H. & Pandolfi, P. P. (2004). PML regulates p53 stability by sequestering Mdm2 to the nucleolus. *Nat Cell Biol* **6**, 665–672.

Borden, K. L. B., Lally, J. M., Martin, S. R., O'Reilly, N. J., Solomon, E. & Freemont, P. S. (1996). In vivo and in vitro characterization of the B1 and B2 zinc- binding domains from the acute promyelocytic leukemia protooncoprotein PML. *Proc Natl Acad Sci U S A* **93**, 1601–1606.

Bourhis, J. M., Johansson, K., Receveur-Brechot, V., Oldfield, C. J., Dunker, A. K., Canard, B. & Longhi, S. (2004). The C-terminal domain of measles virus nucleoprotein belongs to the class of intrinsically disordered proteins that fold upon binding to their physiological partner. *Virus Res* **99**, 157–167.

Callaghan, A. J., Aurikko, J. P., Ilag, L. L., Grossman, J. G., Chandran, V., Kuhnel, K., Poljak, L., Carpousis, A. J., Robinson, C. V. & other authors (2004). Studies of the RNA degradosome-organizing domain of the *Escherichia coli* ribonuclease RNase E. *J Mol Biol* **340**, 965–979.

Carvalho, T., Seeler, J. S., Ohman, K., Jordan, P., Pettersson, U., Akusjarvi, G., Carmofonseca, M. & Dejean, A. (1995). Targeting of adenovirus E1A and E4–ORF3 proteins to nuclear matrix-associated PML bodies. *J Cell Biol* **131**, 45–56.

Condemine, W., Takahashi, Y., Zhu, J., Puvion-Dutilleul, F., Guegan, S., Janin, A. & de The, H. (2006). Characterization of endogenous human promyelocytic leukemia isoforms. *Cancer Res* **66**, 6192–6198.

Condemine, W., Takahashi, Y., Le Bras, M. & de The, H. (2007). A nucleolar targeting signal in PML-I addresses PML to nucleolar caps in stressed or senescent cells. *J Cell Sci* **120**, 3219–3227.

Doucas, V., Ishov, A. M., Romo, A., Juguilon, H., Weitzman, M. D., Evans, R. M. & Maul, G. G. (1996). Adenovirus replication is coupled with the dynamic properties of the PML nuclear structure. *Genes Dev* **10**, 196–207.

Evans, J. D. & Hearing, P. (2003). Distinct roles of the adenovirus E4 ORF3 protein in viral DNA replication and inhibition of genome concatenation. *J Virol* **77**, 5295–5304.

Everett, R. D. & Chelbi-Alix, M. K. (2007). PML and PML nuclear bodies: implications in antiviral defence. *Biochimie* **89**, 819–830.

Everett, R. D. & Maul, G. G. (1994). HSV-1 IE protein Vmw110 causes redistribution of PML. *EMBO J* **13**, 5062–5069.

Everett, R. D. & Murray, J. (2005). ND10 components relocate to sites associated with herpes simplex virus type 1 nucleoprotein complexes during virus infection. *J Virol* **79**, 5078–5089.

Everett, R. D., Rechter, S., Papior, P., Tavalai, N., Stamminger, T. & Orr, A. (2006). PML contributes to a cellular mechanism of repression of herpes simplex virus type 1 infection that is inactivated by ICP0. *J Virol* **80**, 7995–8005.

Everett, R. D., Parada, C., Gripon, P., Sirma, H. & Orr, A. (2008). Replication of ICP0-null mutant herpes simplex virus type 1 is restricted by both PML and Sp100. *J Virol* **82**, 2661–2672.

Fagioli, M., Alcalay, M., Pandolfi, P. P., Venturini, L., Mencarelli, A., Simeone, A., Acampora, D., Grignani, F. & Pelicci, P. G. (1992). Alternative splicing of PML transcripts predicts expression of several carboxyterminally different protein isoforms. *Oncogene* **7**, 1083–1091.

Fagioli, M., Alcalay, M., Tomassoni, L., Ferrucci, P. F., Mencarelli, A., Riganelli, D., Grignani, F., Pozzan, T., Nicoletti, I. & other authors (1998). Cooperation between the RING + B1–B2 and coiled-coil domains of PML is necessary for its effects on cell survival. *Oncogene* **16**, 2905–2913.

Hoppe, A., Beech, S. J., Dimmock, J. & Leppard, K. N. (2006). Interaction of the adenovirus type 5 E4 Orf3 protein with promyelocytic leukemia protein isoform II is required for ND10 disruption. *J Virol* **80**, 3042–3049.

Ishov, A. M. & Maul, G. G. (1996). The periphery of nuclear domain 10 (ND10) as site of DNA virus deposition. *J Cell Biol* **134**, 815–826.

Janderová-Rossmeislová, L., Nováková, Z., Vlasáková, J., Phillmonenko, V., Hozák, P. & Hodný, Z. (2007). PML protein association with specific nucleolar structures differs in normal, tumor and senescent human cells. *J Struct Biol* **159**, 56–70.

Jensen, K., Shiels, C. & Freemont, P. S. (2001). PML protein isoforms and the RBCC/TRIM motif. *Oncogene* **20**, 7223–7233.

Kalderon, D., Roberts, B. L., Richardson, W. D. & Smith, A. E. (1984). A short amino-acid sequence able to specify nuclear location. *Cell* **39**, 499–509.

Kelly, C., van Driel, R. & Wilkinson, G. W. G. (1995). Disruption of PML-associated nuclear bodies during human cytomegalovirus infection. *J Gen Virol* **76**, 2887–2893.

Leppard, K. N. & Dimmock, J. (2006). Virus interactions with PML nuclear bodies. In *Viruses and the Nucleus*, pp. 213–245. Edited by J. Hiscox. Wiley.

Liu, Y., Shevchenko, A. & Berk, A. J. (2005). Adenovirus exploits the cellular aggresome response to accelerate inactivation of the MRN complex. *J Virol* **79**, 14004–14016.

Longhi, S., Receveur-Brechot, V., Karlin, D., Johansson, K., Darbon, H., Bhella, D., Yeo, R., Finet, S. & Canard, B. (2003). The C-terminal domain of the measles virus nucleoprotein is intrinsically disordered and folds upon binding to the C-terminal moiety of the phosphoprotein. *J Biol Chem* **278**, 18638–18648.

Mattsson, K., Pokrovskaja, K., Kiss, C., Klein, G. & Szekely, L. (2001). Proteins associated with the promyelocytic leukemia gene product (PML)-containing nuclear body move to the nucleolus upon inhibition of proteasome-dependent protein degradation. *Proc Natl Acad Sci U S A* **98**, 1012–1017.

Mohan, A. C., Oldfield, C. J., Radivojac, P., Vacic, V., Cortese, M. S., Dunker, A. K. & Uversky, V. N. (2006). Analysis of molecular recognition features (MoRFs). *J Mol Biol* **362**, 1043–1059.

Nevels, M., Tauber, B., Kremmer, E., Spruss, T., Wolf, H. & Dobner, T. (1999). Transforming potential of the adenovirus type 5 E4orf3 protein. *J Virol* **73**, 1591–1600.

Obradovic, Z., Peng, K., Vucetic, S., Radivojac, P. & Dunker, A. K. (2005). Exploiting heterogeneous sequence properties improves prediction of protein disorder. *Proteins* **61** (Suppl. 7), 176–182.

Oldfield, C. J., Cheng, Y., Cortese, M. S., Romero, P., Uversky, V. N. & Dunker, A. K. (2005). Coupled folding and binding with alpha-helix-forming molecular recognition elements. *Biochemistry* **44**, 12454–12470.

Oldfield, C. J., Meng, J., Yang, J. Y., Yang, M. Q., Uversky, V. N. & Dunker, A. K. (2008). Flexible nets: disorder and induced fit in the associations of p53 and 14-3-3 with their partners. *BMC Genomics* **9** (Suppl. 1), S1.

Peng, H. Z., Feldman, I. & Rauscher, F. J., 3rd (2002). Hetero-oligomerization among the TIF family of RBCC/TRIM domain-containing nuclear cofactors: a potential mechanism for regulating the switch between coactivation and corepression. *J Mol Biol* **320**, 629–644.

Romero, P., Obradovic, Z., Kissinger, C. R., Villafranca, J. E. & Dunker, A. K. (1997). Identifying disordered regions in proteins from amino acid sequences. In *IEEE International Conference on Neural Networks*, pp. 90–95.

Romero, P., Obradovic, D., Li, X., Garner, E. C., Brown, C. J. & Dunker, A. K. (2001). Sequence complexity of disordered protein. *Proteins* **42**, 38–48.

Salomoni, P. & Bellodi, C. (2007). New insights into the cytoplasmic function of PML. *Histol Histopathol* **22**, 937–946.

Scaglioni, P. P., Yung, T. M., Cai, L. F., Erdjument-Bromage, H., Kaufman, A. J., Singh, B., Teruya-Feldstein, J., Tempst, P. & Pandolfi, P. P. (2006). A CK2-dependent mechanism for degradation of the PML tumor suppressor. *Cell* **126**, 269–283.

Shen, T. H., Lin, H.-K., Scaglioni, P. P., Yung, T. M. & Pandolfi, P. P. (2006). The mechanisms of PML-nuclear body formation. *Mol Cell* **24**, 331–339.

Sternsdorf, T., Jensen, K. & Will, H. (1997). Evidence for covalent modification of the nuclear dot-associated proteins PML and Sp100 by PIC1/SUMO-1. *J Cell Biol* **139**, 1621–1634.

Stracker, T. H., Carson, C. T. & Weitzman, M. D. (2002). Adenovirus oncoproteins inactivate the Mre11–Rad50–NBS1 DNA repair complex. *Nature* **418**, 348–352.

Stracker, T. H., Lee, D. V., Carson, C. T., Araujo, F. D., Ornelles, D. A. & Weitzman, M. D. (2005). Serotype-specific reorganization of the Mre11 complex by adenoviral E4orf3 proteins. *J Virol* **79**, 6664–6673.

Ullman, A. J. & Hearing, P. (2008). The cellular proteins PML and Daxx mediate an innate antiviral defence antagonized by the adenovirus E4 ORF3 protein. *J Virol* **82**, 7325–7335.

Ullman, A. J., Reich, N. C. & Hearing, P. (2007). Adenovirus E4 ORF3 protein inhibits the interferon-mediated antiviral response. *J Virol* **81**, 4744–4752.

Yondola, M. A. & Hearing, P. (2007). The adenovirus E4 ORF3 protein binds and reorganizes the TRIM family member transcriptional intermediary factor 1 alpha. *J Virol* **81**, 4264–4271.